Solidification and melting of mercury in a porous glass as studied by NMR and acoustic techniques

B. F. Borisov, E. V. Charnaya,* and P. G. Plotnikov
Institute of Physics, St. Petersburg State University, St. Petersburg, 198904 Russia

W.-D. Hoffmann and D. Michel
Faculty of Physics and Geosciences, University of Leipzig, D-04103 Leipzig, Germany

Yu. A. Kumzerov
A.F. Ioffe Physico-Technical Institute RAN, St. Petersburg, 194021, Russia

C. Tien and C.-S. Wur
Department of Physics, National Cheng Kung University, Tainan 701, Taiwan
(Received 14 August 1997; revised manuscript received 27 April 1998)

The melting and freezing phase transitions of mercury in a porous glass were studied by NMR and acoustic techniques. The NMR measurements provided direct information on the total amount of liquid mercury versus temperature. A depression of the phase transition temperatures and pronounced hysteresis between melting and freezing were found. Acoustic measurements showed that the freezing process was irreversible while the melting process consisted of reversible and irreversible temperature ranges. The use of longitudinal and transverse acoustic waves made it possible to obtain information about the origin of reversible and irreversible behavior upon melting. In particular, we found that the complete melting of confined mercury can be acoustically detected using only longitudinal and not transverse waves. The broadening of melting is explained by the formation of a liquid layer on the mercury solid surface, and freezing was driven by the pore geometry with no visible precursor effects. [S0163-1829(98)06033-0]

I. INTRODUCTION

Phase transitions in materials confined within porous glasses are the object of continuing interest. They differ significantly from those in corresponding bulk samples and depend on many factors such as pore size and geometry, wetting, interactions with the inner surface, and so on. Until now, various phase transitions for different materials embedded in porous glasses have been observed experimentally. Recently, the superfluid transition (Refs. 1–4, and references therein), the superconducting phase transition,[5–9] the phase separation in liquids (Refs. 10–12, and references therein), phase transitions in liquid crystals (Refs. 13–16, and references therein), the ferroelectric phase transition,[17] solid-solid phase transitions,[8,18,19] the glass phase transition,[20] the gas-liquid phase transition,[21] and the melting-freezing transitions[3,19,21–38] have been intensively studied. It was found that the interplay of short-range and long-range couplings greatly influences the phase transitions in confined geometries. Size and surface effects for particles in voids as well as the common behavior of the ensemble of particles which form a thoroughly interconnected network within the porous matrix can dominate in particular cases. For example, a lowering of the ferroelectric transition temperature[17] can be treated within the framework of a model for isolated ferroelectric nanoparticles.[39] A smearing-out of the first order nematic-isotropic phase transition in liquid crystals with decreasing pore dimensions[13] is evidently controlled by the pore geometry. However, the sharp superconducting phase transition in porous glasses exhibits strong interconnections between the particles imbedded in the pores.[7]

Among different phase transitions, the melting and freezing phase transitions are of particular interest because they are purely first order and well studied for bulk samples. Various experimental techniques were used for studying the melting and freezing processes in porous glasses including calorimetric, x-ray, and acoustic techniques, electron microscopy, neutron scattering, and NMR. However, most of the previous experiments have been performed for liquid helium,[3,23,26,27,34] water,[36,37] some organic liquids,[19,22,25] oxygen, and some other simple liquids.[24,28,35] The investigations revealed some common features for the melting-freezing phase transitions in restricted geometries such as a lowering of the transition temperatures and pronounced hysteresis between melting and freezing. However, the values of temperature shifts and temperature ranges of freezing and melting varied significantly for particular materials, pore sizes, and geometry. It should be noted that the nature of the hysteresis as well as the physical reasons for observed broadening of melting and freezing is still not clear in spite of numerous studies of the melting-freezing phase transitions in porous media.

Only a few papers are devoted to melting and freezing of confined metals.[29–33,38] For gallium in porous glasses and in an opal-like matrix it was found using NMR and acoustic techniques that freezing occurred sharply when the distribution of pore sizes was narrow and was broadened when the distribution of pore sizes was wide, while melting was broadened for any pore size distribution.[29–32] Both melting

 © 1998 The American Physical Society

and freezing occurred well below the bulk gallium melting point. For indium in a Vycor glass a lowering of temperatures of specific heat peaks associated with melting and freezing was observed[38] and heterogeneous nucleation was suggested. Melting and freezing of mercury in a porous glass was studied using neutron scattering and calorimetric techniques in Ref. 33. In addition to a reduction of the transition temperatures and hysteresis, a strong broadening of both the melting and freezing processes was observed.

On the other hand, melting and freezing of small separated metallic particles have been experimentally studied, most of the papers devoted to melting (Refs. 40 and 41, and references therein). In Ref. 40 a lowering of the melting temperature of small supported gold particles was observed to be roughly proportional to the inverse particle size. Recently, x-ray diffraction and electron microscopy experiments on lead and indium inclusions in aluminum have shown size-dependent superheating and supercooling.[42–44] Although a deep supercooling was also observed for bismuth inclusions in aluminum, melting occurred at or below the bismuth bulk melting point.[45] In Ref. 46 an electron microscopy technique was used for studying the solidification and melting of lead fine particles between two layers of SiO_x. At melting a liquid layer surrounding the solid core was found as a precursor effect while solidification occurred as a fast process with no visible precursor effects. A thermodynamic analysis as well as a computer simulation also predict the appearance of a liquid layer on the solid surface of metallic nanoparticles at melting.[47–49] However, for minute particles one can expect the coexistence of liquid and solid states in some temperature interval.[46,48,50]

In the present paper we report results of NMR and acoustic studies of the melting-freezing phase transition in mercury contained in a porous glass. NMR is especially useful for such studies since it can provide direct data on the amount of gallium in the liquid and solid state.[25,30–32,36,37] Acoustic methods give valuable information about changes in the elastic moduli associated with melting and freezing of confined materials and about stresses and relaxation phenomena in the whole sample.[23,24,29] Note, that combining the NMR and acoustic methods appeared to be fruitful for studies of melting and freezing of gallium in porous glasses.[31]

II. EXPERIMENTAL

The sample under study was prepared from a phase-separated soda borosilicate glass whose pore structure was produced by acid leaching.[51] After acid leaching, an interconnected network of fine pores was formed with the average pore diameter of 7 nm as was determined by mercury intrusion porosimetry. The pore size distribution is fairly narrow with 80% of the pore diameters lying within 0.5 nm of the average size. The liquid mercury was introduced into the porous glass under high pressure up to 10 kbar using the same procedure as for mercury intrusion porosimetry. After filling, when the pressure had been removed, the sample was stable and did not exhibit any substantial weight loss. The mercury volume is about 9% of the total sample volume. The filling factor is about 90% of the total pore volume.

NMR measurements were run using a pulse Bruker MSL 500 NMR spectrometer. The temperature dependence of the ^{199}Hg NMR line in the porous glass has been studied in the temperature range 145–295 K covering the bulk mercury melting point [234.3 K (Ref. 52)]. First the sample under study was cooled from room temperature down to about 145 K and then warmed up again to room temperature. Similar temperature cycles were repeated several times. The rate of warming and cooling was very slow to prevent temperature overshooting, which was in our measurements no more than 0.5 K. Prior to each measurement, the sample was kept at a fixed temperature for about 5 min. The accuracy of temperature control was better than 0.5 K. Furthermore, the sample was held at several fixed temperatures for two hours to study whether this would result in any changes in NMR signals. To detect the intensity of the mercury NMR signal, free induction decays acquired after a single pulse were observed.

Acoustic measurements were performed using the conventional pulse acoustic technique,[53] which gave the relative sound velocity value $\Delta v/v$ with an accuracy of better than 10^{-5} and the relative attenuation coefficient $\Delta\alpha$ with an accuracy within 5%. Temperature dependences of velocity and attenuation for longitudinal and transverse waves were studied. The frequency of longitudinal waves was near 8.5 MHz and that of transverse waves near 5.5 MHz. Repeated cycles of slow cooling and warming similar to those used in the NMR studies were carried out for the sample cut from the same bulk specimen as taken above. The same procedure of holding the sample at a constant temperature for many hours was applied as already described for the NMR. In addition, we measured acoustic velocity and attenuation during partial cycling as will be described in Sec. III to reveal the temperature regions of reversible and irreversible behavior at cooling and warming.

III. RESULTS

The results of the NMR studies for one of the temperature cycles are presented in Fig. 1. It shows the temperature dependence of the integral intensity of the NMR signal which is attributed to liquid mercury. The intensity was measured relative to the integral intensity of the ^{199}Hg NMR line at 295 K. As seen from Fig. 1, the amount of liquid mercury remains constant on cooling from room temperature to about 190 K. A monotonous increasing of the integral intensity in this interval arises due to the normal temperature dependence of magnetic susceptibility. Below 190 K the amount of liquid mercury starts decreasing and vanishes at about 165 K well beyond the melting temperature of the bulk mercury. On warming, hysteresis in the amount of liquid mercury manifests itself; the melting process becomes noticeable above 215 K and ends at the bulk mercury melting temperature. Holding the sample under study at any fixed temperature for more than 2 h has not led to noticeable changes in NMR intensity. The behavior, similar to that shown in Fig. 1, was rather reproducible for other successive temperature cycles. It should be mentioned that we could not find any signal from solid mercury confined within the porous glass in spite of the fact that the ^{199}Hg spin is equal to $\frac{1}{2}$. It should be also noted that when warming was fast enough (with a rate equal to at least 2 K/min), the melting region was shifted to higher temperatures over the bulk mercury melting point.

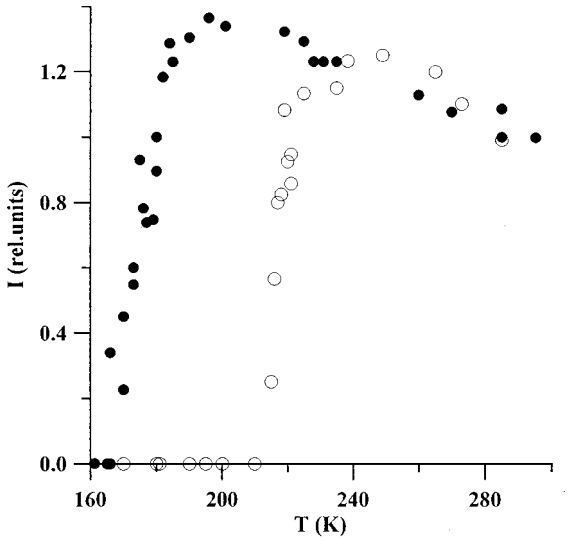

FIG. 1. Intensity I of the ^{199}Hg NMR signal against temperature on cooling (solid circles) and on warming (open circles).

The results of acoustic studies for longitudinal and transverse waves during some of the full temperature cycles are presented in Figs. 2 and 3. As one can see from Figs. 2 and 3, the velocity of longitudinal and transverse ultrasonic waves changes strongly during cooling in the temperature range of about 190 to 165 K, corresponding approximately to the range of decreasing the liquid mercury amount seen by NMR. On warming, there is pronounced hysteresis in both ultrasound velocity and attenuation. The velocity hysteresis loop reaches 1.5% of the velocity value at room temperature for transverse waves and is slightly less for longitudinal waves. The pronounced hysteresis of sound attenuation running up to 7 dB/cm is observed in the same temperature range. Velocity of longitudinal waves starts dropping down at about 195 K, then there is a range of almost linear decrease to 229 K and fast increase to about 234 K [Figure 2(a)]. Above the temperature of bulk mercury melting, the longitudinal ultrasound velocity and attenuation curves associated with cooling and warming are merged together. In contrast, the velocity of transverse waves only decreases monotonously in the range from about 195 to 230 K [Fig. 3(a)]. Above 230 K the transverse ultrasound velocity curves obtained upon cooling and warming are merged similar to the attenuation curves [Fig. 3(b)]. Holding the sample under study at any fixed temperature for more than 15 h has not led to noticeable changes in either ultrasound velocity or attenuation for longitudinal as well as for transverse waves. The behavior of acoustical features similar to that shown in Figs. 2 and 3 was rather reproducible for all other successive temperature cycles. However, a shift of the longitudinal velocity bend to higher temperatures similar to that of confined mercury melting found by NMR and a slight broadening of the bend were observed on fast warming.

To separate the temperature regions of reversible and irreversible behavior of the sample under study upon cooling and warming we performed measurements of longitudinal ultrasound velocity and attenuation during partial temperature cycles. Some of the results are presented in Figs. 4–6. The data obtained have shown that upon cooling the reversible behavior remains until 190 K where velocity starts increasing. Figure 4 shows alterations in velocity during two consecutive cycles, cooling down to 208 K and then warming up to 245 K and cooling down to 197 K and then warming up to 245 K. One can see from Fig. 4 that such partial cycling does not lead to any hysteretic behavior. Increasing velocity in the range between 190–165 K is irreversible. One can see in Fig. 5 that after cooling down to 182 K and subsequently warming up to room temperature the velocity hysteresis loop is within the hysteresis loop for the full temperature cycle. The curves corresponding to partial and full cycles are merged in the range where velocity increases quickly upon warming. On cooling down below 165 K the velocity hysteresis loop no longer depended on the minimal temperature. Upon warming the behavior of the velocity remains reversible until 229 K, this temperature corresponds to the velocity minimum. When warming from low temperatures up to any temperature below 229 K and then cooling down again, the velocity curve reproduces that obtained during warming. To confirm the reversible behavior of the sample under study in this temperature range we performed

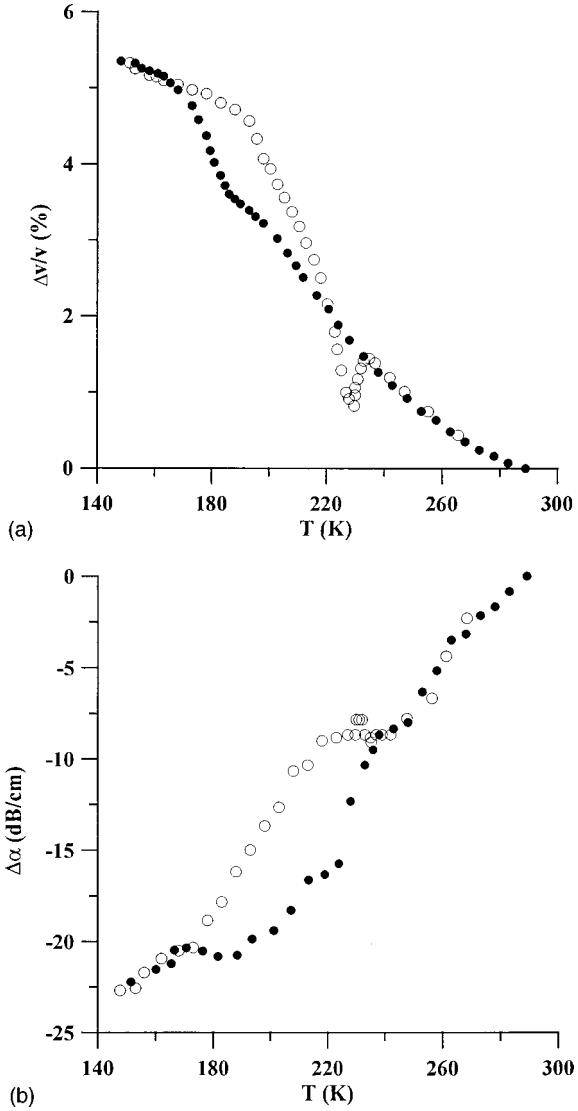

FIG. 2. Longitudinal ultrasound velocity $\Delta v/v$ (a) and attenuation coefficient $\Delta\alpha$ (b) against temperature on cooling (solid circles) and on warming (open circles).

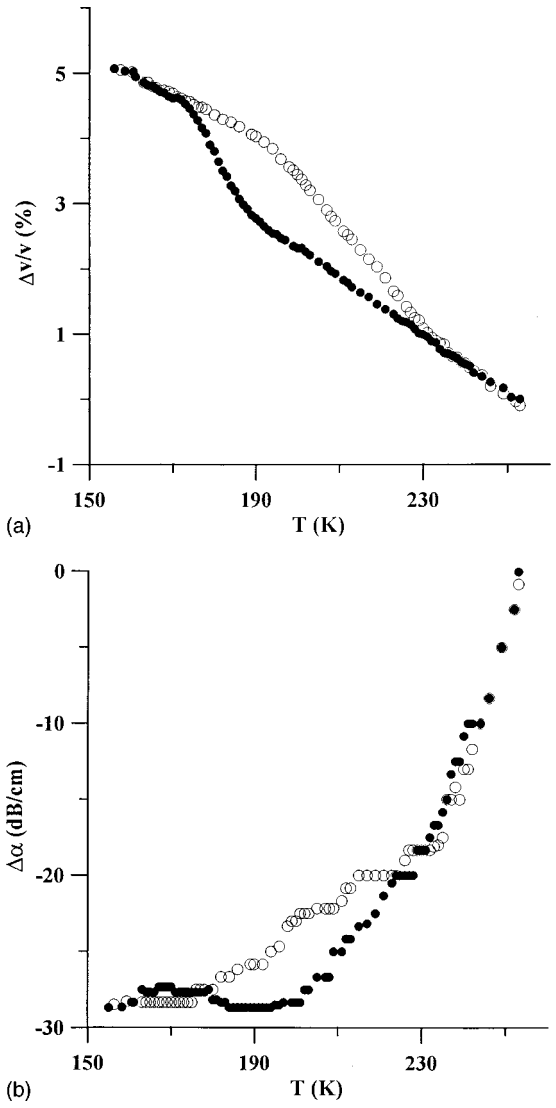

FIG. 3. Transverse ultrasound velocity $\Delta v/v$ (a) and attenuation coefficient $\Delta\alpha$ (b) against temperature on cooling (solid circles) and on warming (open circles).

measurements of sound velocity and attenuation for transverse waves also upon partial cycling below 229 K after cooling to low temperatures. Both the velocity and attenuation curves obtained during cooling and warming coincided within the limits of experimental accuracy. Alterations in velocity between 229 and 234 K are again irreversible as can be seen in Fig. 6. Note that the partial hysteresis loop is within the full one similar to that shown in Fig. 5. Above the temperature of bulk mercury melting where the curves corresponding to cooling and warming are merged, the velocity behavior again becomes reversible. When cooling down from temperatures above 234 K, the velocity curves reproduce that obtained at cooling from room temperature. It should be noted that the behavior of ultrasound attenuation for partial temperature cycles corresponds entirely to that of velocity. An example is shown in Fig. 4.

IV. DISCUSSION

From the thermodynamic point of view, melting in low-dimensional systems is mainly influenced by a large relative

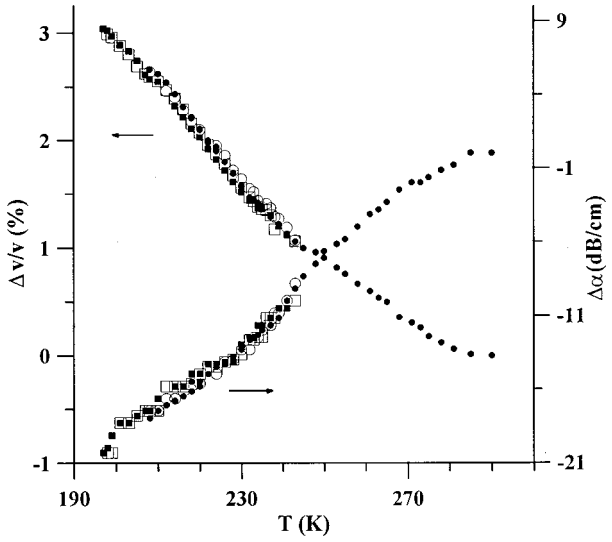

FIG. 4. Longitudinal ultrasound velocity $\Delta v/v$ (left axis) and attenuation coefficient $\Delta\alpha$ (right axis) against temperature taken during partial cycling. First cooling: solid circles, first warming: open circles, second cooling: solid squares, second warming: open squares.

number of surface atoms (that is, by a large surface to volume ratio) and by surface curvature. Since pores form a random interconnected network in porous glasses, the geometry of confined materials is rather complicated. Thus, in most studies of melting and freezing within porous glasses, a model of spherical separated particles or cylinders is used for treating experimental results. Simple theories predict shifts of melting and freezing to low temperatures. Assuming the spherical form of particles within pores, the melting temperature depression ΔT_m is given by the Gibbs-Thompson equation[40,54]

$$\Delta T_m = 4\gamma v_0 T_b / L d, \tag{1}$$

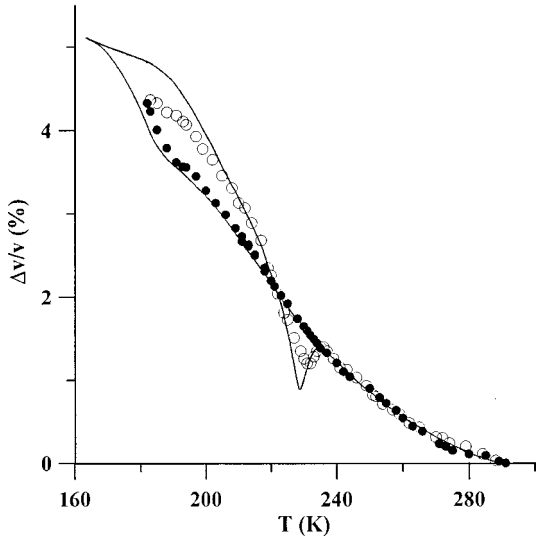

FIG. 5. Longitudinal ultrasound velocity $\Delta v/v$ against temperature on cooling (solid circles) and on warming (open circles). Solid line shows the hysteresis loop for a full temperature cycle.

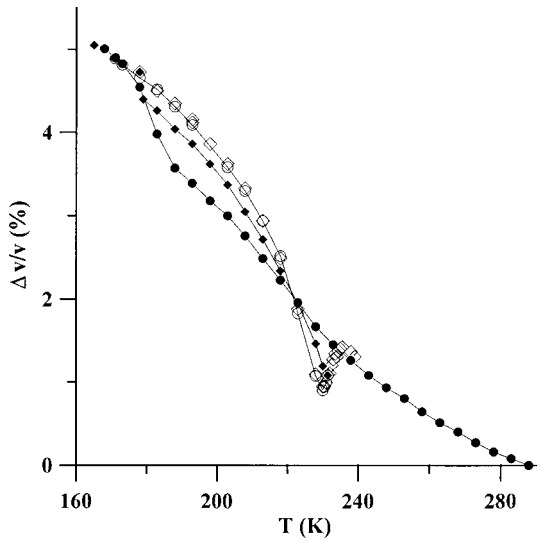

FIG. 6. Longitudinal ultrasound velocity $\Delta v/v$ against temperature taken on cooling from room temperature (solid circles), warming up to 231.5 K (open circles), and on subsequent cooling (solid diamonds) and warming (open diamonds). The solid lines provide a guide for the eye.

where d is the nanoparticle diameter, γ is the surface tension of the solid, L is the latent heat of fusion, T_b is the bulk melting temperature, and v_0 is the molar volume of the solid. Since ΔT_m is related to particle dimensions, the distribution of particle sizes should result in broadening the process of melting. Such an idea was used in some studies to determine small particle and pore size distribution from melting processes.[25,55]

Freezing is normally treated as a result of supercooling. This explains the hysteresis between freezing and melting. Then the freezing process should be mainly controlled by nucleation kinetics and not by the pore geometry. On the other hand, the geometric-freezing model has been discussed for porous media.[24,28] According to this model, freezing in confined nanoparticles is considered similarly to different structural phase transformations.[56] Then it is controlled by pore geometries and the depression of freezing point T_f is given by the following equation:

$$\Delta T_f = 6\alpha v_0 T_b / L d, \tag{2}$$

where α is the surface energy at the liquid-solid interface. However, the geometric-freezing model could not provide an appropriate explanation for the hysteresis.

A more complicated analysis includes a liquid layer surrounding the solid core of a small isolated metallic particle.[49] Some models consider only thermodynamic equilibrium between the molten layer and the solid core at melting.[46,49,55] In others the nucleation rate from the solid or surface melted state is also taken into account (see Ref. 48, and references therein). According to recent theoretical studies the liquid layer should be formed at melting as well as at freezing.[48] For small enough particles, a difference between the melting and freezing temperatures arises then due to different heights of energy barriers for the solid-to-liquid and liquid-to-solid transitions. This implies that the hysteresis loop should depend on the rate of changing temperature. When the barrier becomes very low for minute particles, the difference between melting and freezing should disappear.

For confined liquids which wet the inner surface of porous glasses, using the approximation of spherical particles to treat experimental results does not seem to be quite reasonable. In fact, because of wetting, the interconnection between liquids confined in adjacent pores is not destroyed even in the case of partial filling and such common phenomena might exist as propagating the freezing front along the pore network. However, for mercury which does not wet the glass surface the incomplete pore filling should break down the confined liquid into separated particles. In this case the model of spherical particles seems to be more suitable.

Let us discuss now the results obtained for confined mercury upon freezing and melting. At cooling the NMR and acoustic measurements for longitudinal and transverse waves yield the same result; the freezing occurs within a temperature range of about 25 K starting at about 190 K and ending at about 165 K (Figs. 1–3). The large temperature interval of freezing implies that this process is smeared. Freezing is irreversible in the total range. In contrast, the three methods give different results upon warming the sample. The slopes of the velocity curves start increasing near 195 K for transverse as well as for longitudinal waves (Figs. 2 and 3). However, the velocity curves for transverse waves obtained upon cooling and warming merge near the upper limit of reversible behavior of longitudinal waves, while the velocity of longitudinal waves changes markedly and irreversibly in the range 229 to 234 K. According to NMR, the main amount of mercury melts in the range from 215 K to the melting point of bulk mercury.

To explain all the results obtained, it is necessary to note that transverse and longitudinal ultrasonic waves are sensitive to the structural transformations differently in the sample under study. The elastic modulus for longitudinal waves is combined with the elastic modulus of the glass and that of mercury independently of whether mercury is in solid or liquid state. However, the shear elastic modulus of the sample is combined with those of glass and mercury only when mercury is solid and is just equal to the modulus of the empty glass when mercury is liquid (or there is no mechanical contact between a solid core in pores and the glass matrix because of a liquid skin on the core surface). Taking into account this difference between longitudinal and transverse waves, the results obtained can be treated as follows. Freezing of confined mercury occurs without appearance of a liquid layer on the mercury surface in a temperature range which is much narrower than that of melting. The irreversible behavior upon freezing means that when some amount of mercury solidifies at any intermediate temperature point, it remains solid until warmed up to a rather high temperature near the bulk mercury melting point (Fig. 5) with a hysteresis of about 40 K. This might imply that some number of independent mercury particles became completely solid at some fixed temperature. In any case, the broadening of freezing together with the time independence of the amount of liquid mercury at fixed temperatures on cooling speaks against the crystallization front to be formed within the pore network due to homogeneous nucleation. But these facts and partial

hysteresis loops agree with the suggestion that freezing is driven by heterogeneous nucleation independently in different parts of the sample.

Melting in the temperature range 195 to 229 K is reversible according to acoustic measurements. It can be explained by the formation of a liquid layer on the surface of confined mercury. At lower temperatures the layers surrounding solid cores are thin and maybe not continuous because of irregular pore shape. Thus, they do not prevent completely mechanical contacts between the glass matrix and mercury cores. When warming, these layers become thicker and step by step some pores are excluded from the contribution to the effective shear elastic modulus. Until about 215 K the layers are so thin that they are not registered by NMR, the amount of liquid mercury is smaller than 1% of the total mercury amount. Unfortunately, this interpretation is only qualitative. The quantitative interpretation requires solving the intricate problem of sound propagation through a system of curved liquid and solid irregular layers. This does not allow us to make unambiguous estimates for the liquid skin thickness from acoustic data. At about 229 K the irreversible melting of solid mercury cores begins, the total range of irreversible melting is much narrower than the temperature interval of the liquid skin existence. The overall behavior of confined mercury at melting is in good agreement with that of small separated lead particles.[46] Thus, the melting and freezing processes in confined mercury are very asymmetric. A clear asymmetry in melting and freezing was also recently observed for gallium embedded in porous glasses and an opal-like matrix[29–32] and for fine lead particles between SiO_x layers.[46] This makes it possible to speculate that melting and freezing of confined metals as well as of small metallic particles should be theoretically examined separately.

The above treatment can also be used to explain the broadening of melting and freezing of mercury obtained in Ref. 33. However, the hysteresis between freezing and melting was noticeably narrower in Ref. 33 than in the present paper; the confined mercury was reported in Ref. 33 to be completely melted at 224 K. The difference might have arisen because of different pore geometries. In addition, the temperature of 224 K corresponded in Ref. 33 to the peak in the heat capacity temperature dependence which cannot coincide with the off-set of melting for smeared phase transitions.

It was noted in Sec. III that, upon a fast enough warming the range of melting was shifted to high temperatures above the bulk mercury melting point. Since it is known that the bulk mercury melting point increases with increasing pressure,[52] the increase in temperature for confined mercury on fast warming can be understood as a result of internal pressure which arises because of the difference in thermal expansion for the glass matrix and mercury. The internal pressure corresponding to the observed shift of about 3 K of the mercury melting point can be estimated using results for bulk mercury[52] as 0.7 kbar. This estimate is below the compressive strength of quartz glass.[56]

In conclusion, melting and freezing of mercury confined in a porous glass were studied using NMR and acoustic techniques. The NMR measurements provided direct information on the total amount of liquid mercury versus temperature. A depression of the phase transition temperatures and pronounced hysteresis between melting and freezing were found. A clear asymmetry in freezing and melting was obtained. Acoustic measurements showed that the freezing process was irreversible while the melting process consisted of reversible and irreversible temperature ranges. The use of longitudinal and transverse acoustic waves made it possible to obtain information about the origin of reversible and irreversible behavior upon melting. In particular, it was shown that complete melting of confined mercury can be acoustically detected using only longitudinal and not transverse waves, as was made in most previous studies of melting for confined liquids. Comparison of the NMR and acoustic results allowed us to suggest that a liquid layer was formed on the confined mercury surface upon the reversible melting and the irreversibility range corresponded to the melting of the solid mercury cores.

ACKNOWLEDGMENTS

The present work was in part supported by the Russian Foundation of Fundamental Investigations under Grant No. 96-02-19523, by DFG within the framework of the Innovationskolleg INK 24, and by the National Science Council of Taiwan under Grant No. 86-2112-M-006-012.

*Author to whom correspondence should be addressed. Electronic address: charnaya@brel.spb.su

[1] M. H. W. Chan, K. I. Blum, S. Q. Murphy, G. K. S. Wong, and J. D. Reppy, Phys. Rev. Lett. **61**, 1950 (1988).

[2] D. Finotello, K. A. Gillis, A. P. Y. Wong, and M. H. W. Chan, Phys. Rev. Lett. **61**, 1954 (1988).

[3] J. R. Beamish, A. Hikata, L. Tell, and C. Elbaum, Phys. Rev. Lett. **50**, 425 (1983).

[4] M. Larson, N. Mulders, and G. Ahlers, Phys. Rev. Lett. **68**, 3896 (1992).

[5] M. J. Graf, T. E. Huber, and C. A. Huber, Phys. Rev. B **45**, 3133 (1992).

[6] E. V. Charnaya, Yu. A. Kumzerov, C. Tien, and C. S. Wur, Solid State Commun. **94**, 635 (1995).

[7] E. V. Charnaya, C. Tien, C. S. Wur, and Yu. A. Kumzerov, Physica C **269**, 313 (1996).

[8] C. Tien, C. S. Wur, K. J. Lin, J. S. Hwang, E. V. Charnaya, and Yu. A. Kumzerov, Phys. Rev. B **54**, 11 880 (1996).

[9] E. V. Charnaya, C. Tien, C. S. Wur, and Yu. A. Kumzerov, Physica C **273**, 91 (1996).

[10] S. B. Dierker and P. Wiltzius, Phys. Rev. Lett. **66**, 1185 (1991).

[11] P. Pricaupenko and J. Treiner, Phys. Rev. Lett. **74**, 430 (1995).

[12] S. Lacelle, L. Tremblay, Y. Bussiere, F. Cau, and C. G. Fry, Phys. Rev. Lett. **74**, 5228 (1995).

[13] G. S. Iannacchione, G. P. Crawford, S. Zumer, J. W. Doane, and D. Finotello, Phys. Rev. Lett. **71**, 2595 (1993).

[14] K. Uzelac, A. Hasmy, and R. Jullien, Phys. Rev. Lett. **74**, 422 (1995).

[15] Z. Kutnjak and C. W. Garland, Phys. Rev. E **55**, 488 (1997).
[16] B. Zhou, G. S. Iannacchione, and C. W. Garland, Liq. Cryst. **22**, 335 (1997).
[17] S. V. Pan'kova, V. V. Poborchii, and V. G. Solov'ev, J. Phys.: Condens. Matter **8**, L203 (1996).
[18] D. D. Awschalom and J. Warnock, Phys. Rev. B **35**, 6774 (1987).
[19] R. Mu and V. M. Malhotra, Phys. Rev. B **44**, 4296 (1991).
[20] C. L. Jackson and G. B. McKenna, J. Non-Cryst. Solids **131–133**, 221 (1991).
[21] J. A. Duffy, N. J. Wilkinson, H. M. Fretwell, and M. A. Alam, J. Phys.: Condens. Matter **7**, L27 (1995), and references therein.
[22] C. L. Jackson and G. B. McKenna, J. Chem. Phys. **93**, 9002 (1990).
[23] J. R. Beamish, N. Mulders, A. Hikata, and C. Elbaum, Phys. Rev. B **44**, 9314 (1991).
[24] E. Molz, A. P. Y. Wong, M. H. W. Chan, and J. R. Beamish, Phys. Rev. B **48**, 5741 (1993).
[25] J. H. Strange, M. Rahan, and E. G. Smith, Phys. Rev. Lett. **71**, 3589 (1993).
[26] D. F. Brewer, Cao Liezhao, C. Girit, and J. D. Reppy, Physica B **107**, 583 (1981).
[27] A. L. Thomas, D. F. Brewer, T. Naji, S. Haynes, and J. D. Reppy, Physica B **107**, 581 (1981).
[28] J. Warnock, D. D. Awschalom, and M. W. Shafer, Phys. Rev. Lett. **57**, 1753 (1986).
[29] B. F. Borisov, E. V. Charnaya, Yu. A. Kumzerov, A. K. Radzhabov, and A. V. Shelyapin, Solid State Commun. **92**, 531 (1994).
[30] E. Shabanova, E. V. Charnaya, K. Schaumburg, and Yu. A. Kumzerov, Physica B **229**, 268 (1997).
[31] B. F. Borisov, E. V. Charnaya, W.-D. Hoffmann, D. Michel, A. V. Shelyapin, and Yu. A. Kumzerov, J. Phys.: Condens. Matter **9**, 3377 (1997).
[32] E. Shabanova, E. V. Charnaya, K. Schaumburg, and Yu. A. Kumzerov, J. Magn. Reson., Ser. A **122**, 67 (1996).
[33] Yu. A. Kumzerov, A. A. Nabereznov, S. B. Vakhrushev, and B. N. Savenko, Phys. Rev. B **52**, 4772 (1995).
[34] E. B. Molz and J. R. Beamish, J. Low Temp. Phys. **101**, 1055 (1995).
[35] M. Schindler, A. Dertinger, Y. Kondo, and F. Pobell, Phys. Rev. B **53**, 11 451 (1996).
[36] K. Overloop and L. Vangerven, J. Magn. Reson., Ser. A **101**, 179 (1993).
[37] Y. Hirama, T. Takahashi, M. Hino, and T. Sato, J. Colloid Interface Sci. **184**, 349 (1996).
[38] K. M. Unruh, T. E. Huber, and C. A. Huber, Phys. Rev. B **48**, 9021 (1993).
[39] W. L. Zhong, Y. G. Wang, P. L. Zhang, and B. D. Qu, Phys. Rev. B **50**, 698 (1994).
[40] Ph. Buffat and J.-P. Borel, Phys. Rev. A **13**, 2287 (1976).
[41] R. Kofman, P. Cheyssac, and R. Garrigos, Phase Transit. **24–26**, 283 (1990).
[42] H. Saka, Y. Nishikawa, and T. Imura, Philos. Mag. A **57**, 895 (1988).
[43] L. Gråbek, J. Bohr, H. H. Andersen, A. Johansen, E. Johnson, L. Sarholt-Kristensen, and I. K. Robinson, Phys. Rev. B **45**, 2628 (1992).
[44] L. Gråbek, J. Bohr, E. Johnson, A. Johansen, L. Sarholt-Kristensen, and H. H. Andersen, Phys. Rev. Lett. **64**, 934 (1990).
[45] N. B. Toft, J. Bohr, B. Buras, E. Johnson, A. Johansen, H. H. Andersen, and L. Sarholt-Kristensen, J. Phys. D **28**, 539 (1995).
[46] T. Ben David, Y. Lereah, G. Deutsher, R. Kofman, and P. Cheyssac, Philos. Mag. A **71**, 1135 (1995).
[47] F. Ercolessi, W. Andreoni, and T. Tosatti, Phys. Rev. Lett. **66**, 911 (1991).
[48] R. R. Vanfleet and J. M. Mochel, Surf. Sci. **341**, 40 (1995).
[49] P. R. Couchman and W. A. Jesser, Nature (London) **269**, 481 (1977).
[50] R. S. Berry and D. J. Wales, Phys. Rev. Lett. **63**, 1156 (1989).
[51] *Two-phase Glasses: Structure, Properties, Applications*, edited by B. G. Varshal (Nauka, Leningrad, 1991) (in Russian).
[52] D. C. Wallace, Proc. R. Soc. London, Ser. A **439**, 177 (1992).
[53] E. V. Charnaya and I. Rakhimov, Ferroelectrics **112**, 45 (1990).
[54] P. Pawlow, Z. Phys. Chem., Stoechiom. Verwandtschaftsl. **65**, 545 (1909).
[55] C. R. M. Wronski, Br. J. Appl. Phys. **18**, 1731 (1967); I. D. Morokhov, L. I. Trusov, and V. N. Lapovok, *Physical Phenomena in Ultradispersed Media* (Energoatomizdat, Moscow, 1984) (in Russian).
[56] *CRC Handbook of Chemistry and Physics*, edited by R. C. Weast (CRC, Boca Raton, FL, 1980).